



Case Report

Volume 23 Issue 4 - April 2023
DOI: 10.19080/CTOIJ.2023.23.556119

Cancer Ther Oncol Int J

Copyright © All rights are reserved by Dr. Isabel Sollozo-Dupont

Magnetic Resonance Imaging (MRI) of Metastatic Scalp, Skull and Dural Tumors in a Case of Ewing's Sarcoma, with Literature Review



Reyes-Pérez Juan Armando¹, Jiménez- De Los Santos Mayra Evelia¹, Vidaurre-Herrera Clara Alejandra¹, Villaseñor Navarro Yolanda¹, Pacheco-Bravo Irlanda¹, Salazar-López Alejandro¹, Martínez Tlahuel Jorge Luis², Cano-Valdez Ana Maria³ and Sollozo-Dupont Isabel^{1*}

¹Department of Radiology and Imaging, Instituto Nacional de Cancerología, INCan, México

²Department of Medical Oncology, Instituto Nacional de Cancerología, INCan, México

³Department of Surgical Pathology, Instituto Nacional de Cancerología, INCan, México

Submission: March 27, 2023; **Published:** April 10, 2023

***Corresponding author:** Dr. Isabel Sollozo-Dupont, Department of Radiology and Imaging, Instituto Nacional de Cancerología, Av. San Fernando No. 22, Col. Sección XVI Delegación Tlalpan, CDMX, C.P.14080 México

Abstract

The prognosis of patients with initially metastatic ES is very poor. Significant risk factors for death include affectation at combined local and distant sites and soft tissue involvement. For the diagnosis, an initial radiographic and/or computed tomography (CT) is performed. Both techniques are outstanding in evaluating the affected bones. However, when primary Ewing's tumor or its metastases involves soft tissues, these might be misdiagnosed if magnetic resonance imaging (MRI) is not applied. The purpose of the present case is to expose the role of MRI in the assessment of a rare and aggressive ES with metastases affecting bones and soft tissue of the head.

Keywords: Advanced Ewing sarcoma; Scalp and skull metastases; Magnetic resonance imaging

Abbreviations: ALP: Alkaline Phosphatase; ALT: Alanine Aminotransferase; CNS: Central nervous system; CT: Computer Tomography; ES: Ewing Sarcoma; GGT: Gamma-glutamyl transferase; LDH: Lactic Acid Dehydrogenase; MRI: Magnetic Resonance Imaging; WI: Weighted Imaging

Introduction

Ewing's sarcoma (ES) is the second most common bone tumor after osteosarcoma in children and adolescents [1-3]. The frequency of ES is 1-3 per million per year in the Western hemisphere, with a slight predominance in men [4,5]. Although its etiology is largely unknown, some conditions are linked with a high risk of malignant degeneration, including radiation injury and benign cartilaginous dysplasia's (Ollier disease, Maffucci syndrome) [6]. Main symptoms include pain, swelling, general discomfort, movement limitation, hyperthermia of the skin, weight loss, pathologic fractures and alteration of anatomic profile with a visible mass [7-9]. Similar to several other sarcomas, ES displays aggressive behavior with a tendency towards recurrence following resection and pronounced proclivity toward early hematogenous metastases to lung and bone [10,11]. For the initial evaluation, a conventional radiography, as well as a computed

tomography (CT) examination, is performed. Both techniques reveal aggressive features such as bone destruction with a moth-eaten to permeative pattern and a wide zone of transition [12]. Currently, there is an increasing demand to include magnetic resonance imaging (MRI) in the management of patients with the suspicion of advanced ES [13-16]. The role of MR imaging is to afford recognition of these lesions that need further aggressive work-up, excluding all others. The definite role of MR imaging in grading soft tissue tumors seems to have become established. As for grading, a lot of individual imaging characteristics used for tissue characterization have low sensitivity, but combinations of parameters (age, site, signal intensities) are more useful and often allow to predict a specific diagnosis or to narrow down the list of differential diagnoses. The soft tissue involvement in the advanced ES is frequent and can be detected accurately by MRI [17].

Originally, ES was treated with radiation or surgery alone with a high fatality rate. In the last three decades, with the addition of chemotherapy, the prognosis of ES has steadily improved, with 5-years survival rates of 60 to 70% for patients with localized disease [18]. Unfortunately, survival for patients with initially metastatic disease remains poor, with 5-year survival rates of 15 to 33% [19,20]. Although prognostic factors are currently discussed, some authors propose primary pelvic tumor and metastatic soft tissue involvement as the most important factors increasing the risk for death [6,19-21].

Here, we present an 18-year-old Mexican female with a palpable large mass of ES in the right knee and metastases involving multiple organs that were identified by CT and MRI. Disease extension includes soft tissue lesions away from the primary tumor (scalp), which could be underestimated in the absence of MRI. This technique also documents skull metastases, and the infiltrated dura, which is highly aggressive and therefore cannot be cured with surgery. Since scalp metastasis in ES may herald the diagnosis of internal malignancy in the head, with the present case we attempt to expose the additional diagnostic value of MRI to evaluate soft tissue involvement, particularly in patients with potential compromise of the central nervous system (CNS) [22,23].

Case presentation

An 18-year-old healthy Mexican female presented with a 9-months history of pain and increased knee volume. Extra-institutional histopathological analysis found a small, blue, round cell tumor, which was poorly differentiated (high grade). Bone tissue involvement, accompanied with neuroendocrine differentiation and intense stromal sclerosis, was also reported. Clinical examination revealed normal motor strength, sensory function and reflexes. Musculoskeletal examination

also was within normal limits without tenderness of the hips or back. On palpation, there was a tumor of approximately 8 cm in diameter on the right knee. An intense right costal pain as an intermittent sharp stabbing was referred by the patient. Also, physicians noticed two swellings over the scalp approximately 3 cm in diameter. These lesions were mostly asymptomatic except for occasional pain due to trauma induced by combing. There was no history of preceding trauma and none of the other family members had a similar complaint.

A simple CT with both soft tissue and bone window an aggressive-looking cortical bone erosion in the epiphysis of the tibia with a “sun ray” speculation pattern given a marked periosteal reaction, with extension into soft tissue (Figure 1 A-D). In addition, a single regional lymph node was demonstrated on the right popliteal fossa showed soft tissue lesions on the third segment of both costal arches (right and left). Other noticeable tumors were on dorsal paravertebral tissues (Figure 2A-B). Such bone lesions were accompanied by multiple round hypodense liver masses (Figure 2C). Subsequently, magnetic resonance imaging (MRI) was used for the evaluation of scalp lesion. Gradient echo sequences showed cranial vault thickening in the diploe (inner table) and “brush appearance” of the bone, which was adjacent to frontoparietal regions and zygomatic arch (Figure 3A-B). A solid area with restricted diffusion suggesting dural infiltration was also revealed (Figure 3C). On the other hand, contrasted T1W images demonstrated a superficial lesion of the soft tissue affecting the left frontoparietal lobe, which was adjacent to the superior sagittal venous sinus (Figure 4A-B). Moreover, blurry grooves and fissures were noticed, which were related to brain swelling (Figure 4B). Meanwhile, T2W images also show hypointense diploe thickening as well as a superficial soft-tissue lesion, which was previously described in contrasted T1W image (Figure 5).

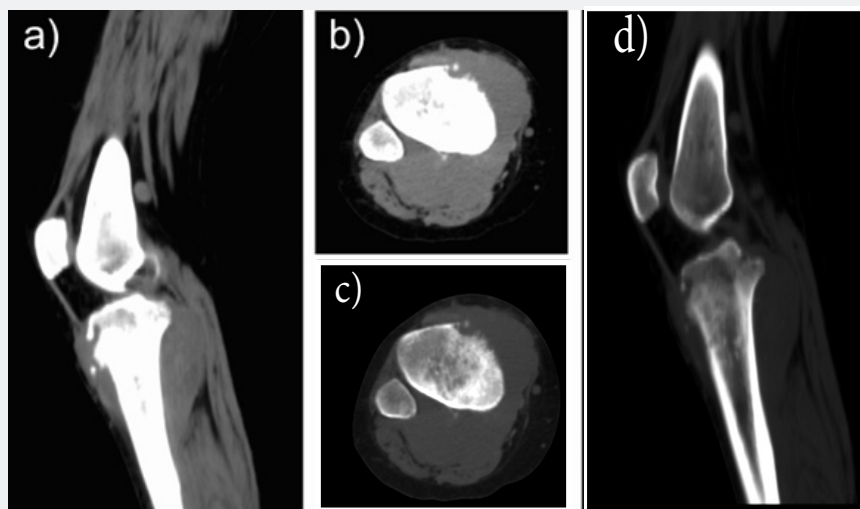


Figure 1: Different window settings of right knee CT scan demonstrating increased soft tissue volume on the proximal epiphysis of the tibia and a single regional node on the right popliteal fossa (A-B which are images from soft tissue window), as well as bone erosion and “sun ray” periosteal reaction (C-D which are images from bone window).

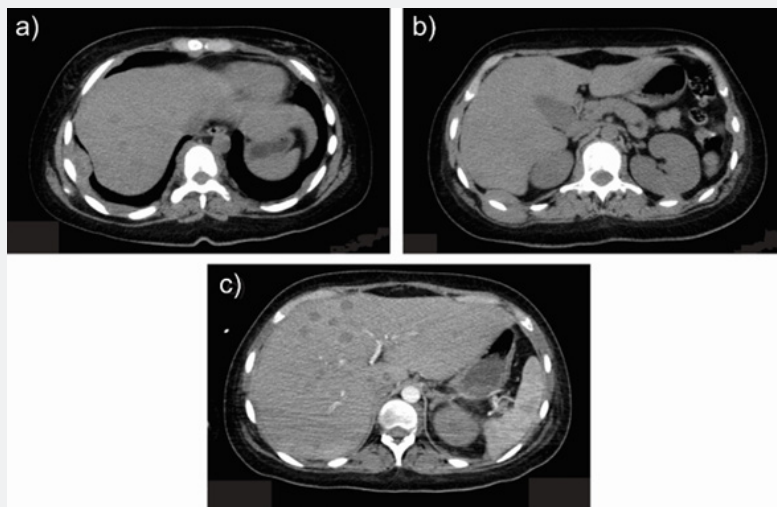


Figure 2: Axial reconstruction from abdominal CT which shows nodular pleural thickening associated with both costal and paravertebral soft tissue thickening (A). A mass surrounding the right costal arch is also demonstrated, as well as hypodense masses in the left lobe of the liver (hepatic segment IVA) (B). Finally, multiple hypodense nodular lesions distributed in both hepatic lobes are distinguished in arterial phase (AP) scan (C).

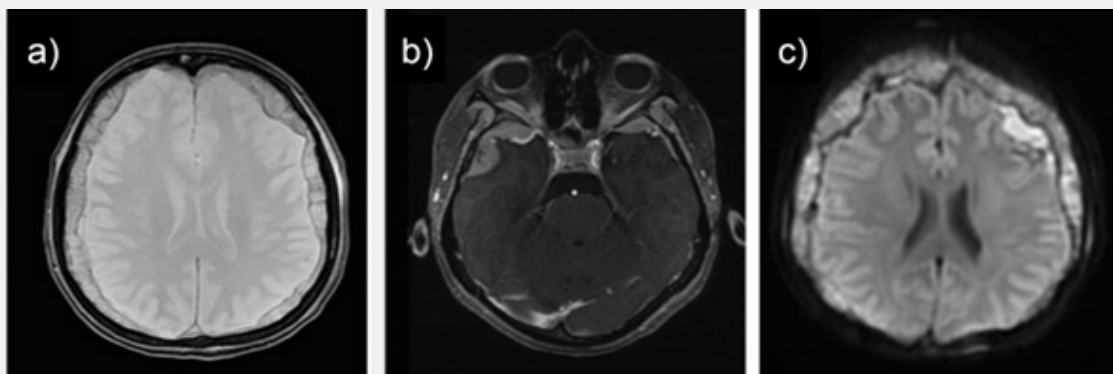


Figure 3: Gradient-echo image showing thickening of the diploe (inner table) and extreme "brush pattern" (A). Axial sequence of MRI T1W images (with gadolinium) showing a tumor spreading the zygomatic arches (B). Diffusion image demonstrating thickening of the diploe and restricted diffusion, which were associated to a left frontal subdural component (C).

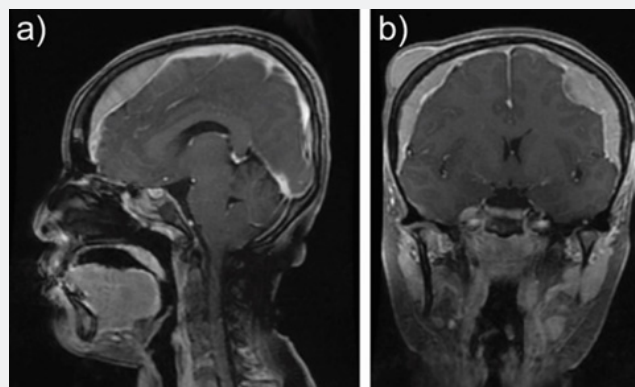


Figure 4: Sagittal (A) and coronal (B) TIW images (with gadolinium) showing a thickened diploe (inner table) having a significant frontal predominance. The displacement of the anterior third of superior sagittal sinus is noticed, as well as a displacement of meninges from their normal position.

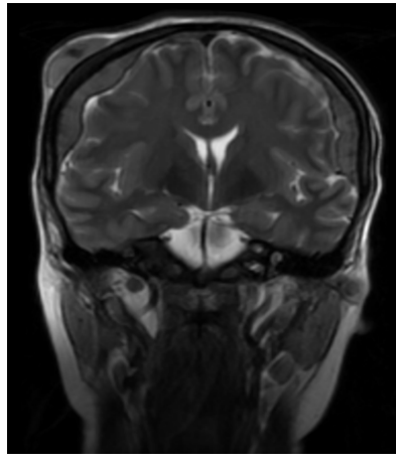


Figure 5: T2-weighted image showing a hypointense diploic thickening as well as a right subcutaneous mass.

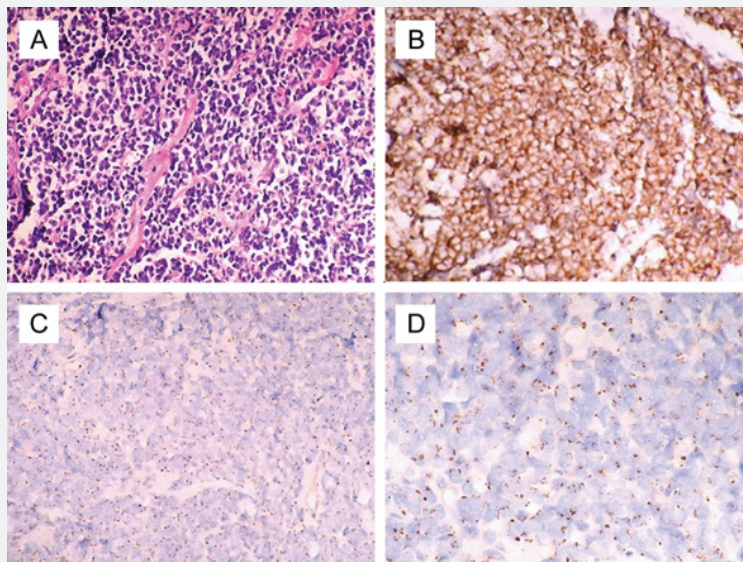


Figure 6: Hematoxylin and eosin (H&E) stains -100 X- showing round cell neoplasm with scant cytoplasm grouped in nests that are from the connectivity tissue, with few thin-walled vessels (A). Also, it is showed immunohistochemistry with anti-synaptophysin antibody -100x- (B), and intense and diffuse cytoplasmatic expression of CD-99 -100x (C)- and -400x (D).

Laboratory assessments suggested an increased liver function. For example, lactic acid dehydrogenase (LDH, 4025 U/L), ALT (149 U/L), GGT (222 U/L) and alkaline phosphatase (ALP, 162 mg/dL). Remarkably, the patient had low hemoglobin levels as well (7.8 g/dL). An initial core needle biopsy of the scalp lesions revealed a small, round blue cell neoplasm, suggestive of a primitive neuroectodermal tumor. The tumor was markedly positive for vimentin and CD-99 (TLE-1, CDE-99), like the prior knee biopsy (Figure 6A-D). With these findings, a diagnosis of ES stage IV (T3N0M1) was completed. The patient was treated with vincristine 183 mg/m², doxorubicine 114 mg/m², cyclophosphamide 1524 mg/m². Unfortunately, she died two months after the first cycle of chemotherapy.

Discussion

ES is a highly malignant bone tumor that usually arises from long bones and soft tissues in the second decade of life [24-26]. The overall incidence of ES seems to remain unchanged in the last thirty years, with an average of 2.93 cases/1,000,000 reported annually [5,16]. In 90% cases, it is seen in patients less than 20 years of age, the highest incidence being observed in 5-13-year-old patients [27]. Metastatic disease is the most unfavorable prognostic feature for ES patients. As stated by Rana et al. and Valdes et al. [27,28] distant metastasis usually involves the lung (38%), bone (including the spine; 31%) and the bone marrow (11%). Metastases to skull bones are seen in approximately 9%

of cases, only a few cases being reported in literature till date [29]. Dural metastases have also been described with ES in a very limited number of cases [30,31].

Demographic distribution of patients with bone metastasis demonstrated only 10% having solitary metastasis, while 25% had 2–5 lesions and 44% had more than five bone metastases, thus limiting the numbers to less than one-third who would have long-term outcomes with aggressive chemotherapy and local radiotherapy [29]. Blood or biochemical tests are nonspecific and inadequate to obtain an accurate diagnosis. Nonspecific signs of tumor, such as an elevated sedimentation rate, moderate anemia, or leukocytosis, may be noted [32]. The computed tomography features of Ewing's sarcoma in our case were those of classic Ewing's sarcoma: a destructive lesion with bone expansion and a sunray periosteal reaction on the proximal epiphysis of the tibia.

Pain and swelling on top of the head were the reasons why an MRI of the brain was performed in our patient, showing metastasis to both diploe and dura. A soft tissue mass overlying the scalp was noticed as well. About MRI features from diploe and dura metastases, the literature indicates that these usually deviate low to intermediate signal intensity on both T1W and T2W, as in the present case. Additionally, an avid enhancement after gadolinium administration and restricted diffusion was noticed [33–35]. According with Saifuddin et al. soft tissue masses are seen in 87% of the reported cases with diploe affection. These are demonstrated as areas of high signal intensity on T2W [36].

To the best of our knowledge, the case reported here is one of the few cases in the English medical literature highlighting the MRI application in the assessment of ES with aggressive metastases involving the scalp, skull and dura. We consider that major morphological findings by MRI were the location and size of scalp lesions, and their extension. Undoubtedly, the picture was completed by evidencing the diploe thickening for which infiltration over the subdural space was noticed. All these features might be misdiagnosed without MRI. Interestingly, neither signs nor symptoms of neurological compromise were noticed in the overall clinical assessment. However, a few days after imaging evaluation, the patient coursed with seizures because of insults perturbing brain function.

As mentioned earlier, metastasis in patients with ES is clinically detectable in up to 34% of the patients at the time of initial diagnosis. Even in those patients with apparently localized primary tumors, the median time from initial treatment to the development of detectable metastasis ranges from only 4 to 12 months when treatment is confined to the primary site. Metastasis characteristically occurs to the lung and skeletal system with equal frequency, other sites being involved in less than 10% of cases. Central nervous system spread is rare as patients do not survive long enough except where early treatment has been instituted [37]. For these advanced stages, median duration of survival is about 3 months [38,39].

Diagnosis and therapeutic management can be challenging. As mentioned earlier, the treatment includes various combinations of surgery, chemotherapy (multiagent chemotherapy regimen) and radiation therapy. Adjuvant and/or neoadjuvant chemotherapy may affect overall survival and improve the treatment results in the future. Some studies have reported that ES can respond dramatically to initial therapy, with robust initial responses predicting a better outcome [40,41]. Unfortunately, neither surgical options nor neoadjuvant chemotherapy achieved a significant survival benefit in our patient by his metastases.

In conclusion, at present, ES remains a lethal disease process whose prognosis largely depends on its stage at the time of presentation. There is evidence indicating that patients presenting tumors >8 cm usually have metastatic disease [26]. Also, decreased socioeconomic status and limited access to health care are factors that affect survival [2]. When all these factors converge, as in the present case, MRI appears to be a responsive alternative identifying metastatic lesions, and the widespread use of this imaging technique would increase the accuracy for determining ES staging, including preoperative surgical planning.

Conclusion

Metastatic ES involving head is an aggressive condition which contribute to death. Due to there are few cases reported in the English medical literature describing cranial metastasis of ES, its imaging features are relative unknown. However, it is usually reported that this metastasis affects bone and the adjacent soft tissue, by which MRI is commonly indicated. MRI has proven to be outstanding evaluating a variety of soft tissue including the scalp. Thus, this technique is emerging for the initial assessment of ES patients having associated swelling on head.

Acknowledgement

We thank Dulce Lupita Mejía Ríos and Elena Minerva Melo García for participating in the critical revision of the final work.

Funding

No external support (financial or in-kind) was received for the completion of this project.

Data Availability

Additional data such as full DICOM images are available from the corresponding author upon request.

Conflicts of Interest

The authors declare that they have no conflicts of interest.

Consent for publication

Written informed consent was obtained from the patient for publication of this case report.

References

- NJ Balamuth, RB Womer (2010) Ewing's sarcoma. *The Lancet Oncology*. 11(2): 184-192.
- MB McCarville, JY Chen, JL Coleman, Yimei Li, Xingyu Li, et al. (2015) Distinguishing Osteomyelitis From Ewing Sarcoma on Radiography and MRI. *AJR Am J Roentgenol* 205(3): 640-651.
- T Ozaki (2015) Diagnosis and treatment of Ewing sarcoma of the bone: a review article. *J Orthop Sci* 20(2): 250-263.
- N Riggi, I Stamenkovic (2007) The Biology of Ewing sarcoma. *Cancer Letters* 254(1): 1-10.
- N Esiashvili, M Goodman, RB Jr. Marcus (2008) Changes in incidence and survival of Ewing sarcoma patients over the past 3 decades: Surveillance Epidemiology and End Results data". *Journal of Pediatric Hematology/ Oncology* 30(6): 425-430
- FR Evola, L Costarella, V Pavone, Giuseppe Caff, Luca Cannavò, et al. (2017) Biomarkers of Osteosarcoma, Chondrosarcoma, and Ewing Sarcoma. *Frontiers in pharmacology* 8: 150.
- FR Singer, DR Eyre (2008) Using biochemical markers of bone turnover in clinical practice. *Cleve Clin J Med* 75(10): 739-750.
- MU Jawad, SP Scully (2010) In brief: classifications in brief: enneking classification: benign and malignant tumors of the musculoskeletal system". *Clinical Orthopaedics and Related Research* 468(7): 2000-2002.
- K Szuhai, AM Cleton-Jansen, PC Hogendoorn, Judith V M G Bovee (2012) Molecular pathology and its diagnostic use in bone tumors. *Cancer genetics* 205(5): 193-204.
- W Khaliq, MF Bahador, T Nichols Laurence, Ronald Andrew Sapiente (2012) Ewing's sarcoma: A case report of a 52-year-old woman with recurrent tumor and literature review. *Oncology letters* 3(1): 155-158.
- M Brotzmann, F Hefti, D Baumhoer (2013) Do Malignant Bone Tumors of the Foot Have a Different Biological Behavior than Sarcomas at Other Skeletal Sites?". *Sarcoma* 2013: 767960.
- MD Murphey, LT Senchak, PK Mambalam, Chika I Logie, Mary K Klassen-Fischer, et al. (2013) From the radiologic pathology archives: ewing sarcoma family of tumors: radiologic-pathologic correlation. *Radiographics* 33(3): 803-831.
- H Jalal, Z Belhadj, H Enneddam, Mohammed Madhar, Tarik Fikry, et al. (2011) Contribution of magnetic resonance imaging in the diagnosis of talus skip metastases of Ewing's sarcoma of the calcaneus in a child: a case report. *J Med Case Rep* 5: 451.
- I Lloret, A Server, I Taksdal (2009) Calvarial Lesions: A Radiological Approach to Diagnosis. *Acta Radiologica* 50(5): 531-542.
- R Van Dams, Henry S Park, Ahmed K Alomari, Adele S Ricciardi, Hari-ni Rao, et al. (2016) Adjuvant hypofractionated partial-brain radiation therapy for pediatric Ewing sarcoma brain metastases: case report. *J Neurosurg Pediatr* 4(17): 434-438.
- C Frouge, D Vanel, C Coffre, D Couanet, G Contesso, et al. (1988) The role of magnetic resonance imaging in the evaluation of Ewing sarcoma. *Skeletal Radiology* 17(6): 387-392.
- A De Schepper, L De Beuckeleer, J Vandevenne, J Somville (2000) Magnetic resonance imaging of soft tissue tumors. *European Radiology* 10(2): 213-223.
- DB Zobel, D Vanel, C Coffre, D Couanet, G Contesso, et al. (2014) The role of Imaging in Ewing sarcoma. *Skeletal Radiol* 17(6): 387-392.
- RM Wilkins, DJ Pritchard, EB Omer, et al. (1986) Ewing's sarcoma of bone: experience with 140 patients. *Cancer* 58(11): 2551-2555.
- R Ladenstein, U Potschger, MC Le Deley, Jeremy Whelan, Michael Paulussen, et al. (2010) Primary disseminated multifocal Ewing sarcoma: results of the Euro-EWING 99 trial. *J Clin Oncol* 28(20): 3284-3291.
- P Picci, T Bohling, G Bacci, S Ferrari, L Sangiorgi, et al. (1997) Chemotherapy-induced tumor necrosis as a prognostic factor in localized Ewing's sarcoma of the extremities. *J Clin Oncol* 15(4): 1553-1559.
- J Huh, KW Kim, SJ Park, Hyoung Jung Kim, Jong Seok Lee, et al. (2015) Imaging Features of Primary Tumors and Metastatic Patterns of the Extraskeletal Ewing Sarcoma Family of Tumors in Adults: A 17-Year Experience at a Single Institution. *Korean J Radiol* 16(4): 783-790.
- II Oz, I Serifoglu, E Bozay Oz, Piskin E, Edebalı N, et al. (2015) Sarcoma: Dural Metastases after Intracranial Hemorrhage. *Pediatric Neurosurgery* 50: 48-52.
- S Cotterill, L Parker, A Malcolm, M Reid, L More, et al. (2000) Incidence and survival for cancer in children and young adults in the North of England, 1968-1995: a report from the Northern Region Young Persons' Malignant Disease Registry. *Br J Cancer* 83(3): 397-403.
- JP Ginsberg, P Goodman, W Leisenring, Kirsten K Ness, Paul A Meyers, et al. (2010) Long-term Survivors of Childhood Ewing Sarcoma: Report from the Childhood Cancer Survivor Study. *J Natl Cancer Inst* 102(16): 1272-1283.
- KR Duchman, Y Gao, BJ Miller (2015) Prognostic factors for survival in patients with Ewing's sarcoma using the surveillance, epidemiology, and end results (SEER) program database. *Cancer Epidemiology* 39(2): 189-195.
- K Rana, V Wadhwa, EK Bhargava, Vasun Batra, Shramana Mandal, et al. (2015) Ewing's Sarcoma Multifocal Metastases to Temporal and Occipital Bone: A Rare Presentation. *J Clin Diagn Res* 9(6): MD04-5.
- M Valdes, G Nicholas, S Verma, Timothy Asmis (2017) Systemic Therapy Outcomes in Adult Patients with Ewing Sarcoma Family of Tumors. *Case Rep Oncol* 10(2): 462-472.
- N Khanna, A Pandey, J Bajpai (2017) Metastatic Ewing's Sarcoma: Revisiting the Evidence on the Fence. *Indian J Med Paediatr Oncol* 38(2): 173181.
- II Oz, I Serifoglu, E Bozay Oz, Piskin E, Edebalı N, et al. (2015) Sarcoma: Dural Metastases after Intracranial Hemorrhage. *Pediatric Neurosurgery* 50: 48-52.
- AB Nsir, M Boughamoura, M Maatouk, et al. (2013) Dural metastasis of Ewing's sarcoma". *Surgical neurology international* 4(96).
- S Ozturk, E Kurtulus Ozturk, N Isiksalan Ozbulbul, Berat Acu, Emine Dundar, et al. (2021) Primary Extraosseous Ewing's Sarcoma of the Lung: Radiologic and Pathologic correlation. *The Cureus Journal of medical Science* 13(5): e14830.
- W Hou, L Xu, H Zhan, et al. (2017) Computed Tomography and Magnetic Resonance Imaging Characteristics of Peripheral Primitive Neuroectodermal Tumor: A Retrospective Analysis of 16 Cases. *Journal of Computer Assisted Tomography* 2(41).
- JL De Sa Neto, MN Simao, MD Crema, Edgard Eduard Engel, Marcello Henrique Nogueira-Barbosa, et al. (2017) Diagnostic performance of magnetic resonance imaging in the assessment of periosteal reactions in bone sarcomas using conventional radiography as the reference. *Radiologia Brasileira* 3(50): 176-181.
- A Mathur, N Jain, C Kesavadas, et al. "Imaging of skull base pathologies: Role of advanced magnetic resonance imaging techniques". *The Neuroradiology Journal*. vol. 28. núm. 4. pages 426-437. 2015.

36. MSAH Saifuddin, CY Ng, MS Abdullah (2021) Skull Base Primary Ewing Sarcoma: A Radiological Experience of a Rare Disease in an Atypical Location. American Journal of Case Reports 22: e930384.
37. Dori Woldu, Daniel Zewdneh, Yocabel Gorfu, Daniel Admasie, (2020) Ewing sarcoma with unusual skull metastasis in a 4-year-old female child: A case report from East Africa. Ethiop Med J 58(1).
38. S Parasuraman, J Langston, BN Rao, C A Poquette, J J Jenkins, et al. (1999) Brain metastases in pediatric Ewing Sarcoma and Rhabdomyosarcoma: The St Jude children's research hospital Experience. J Pediatr Hematol Oncol 21(5): 370-377.
39. G Cugati, M Singh, A Pande, Nigel Peter Symss, Vasudevan M Chakravarthy, et al. (2013) Isolated skull base primary Ewing's sarcoma: An extremely rare location. J Cancer Res Ther 9(4): 741-742.
40. N Gaspar, DS Hawkins, U Dirksen, Ian J Lewis, Stefano Ferrari, et al. (2015) Ewing Sarcoma: Current Management and Future Approaches Through Collaboration. J Clin Oncol 33(27): 3036-3046.
41. DN Friedman, K Chastain, JF Chou, Chaya S Moskowitz, Roberto Adsuar, et al. (2017) Morbidity and mortality after treatment of Ewing sarcoma: A single-institution experience. Pediatric Blood & Cancer 64(11).



This work is licensed under Creative Commons Attribution 4.0 License
DOI: [10.19080/CTOIJ.2023.23.556119](https://doi.org/10.19080/CTOIJ.2023.23.556119)

**Your next submission with Juniper Publishers
will reach you the below assets**

- Quality Editorial service
- Swift Peer Review
- Reprints availability
- E-prints Service
- Manuscript Podcast for convenient understanding
- Global attainment for your research
- Manuscript accessibility in different formats
(Pdf, E-pub, Full Text, Audio)
- Unceasing customer service

Track the below URL for one-step submission

<https://juniperpublishers.com/online-submission.php>